

# More on phase diagram of Laponite

B. Ruzicka<sup>1,2</sup>, L. Zulian<sup>2,3</sup>, G. Ruocco<sup>1,2</sup>

<sup>1</sup> *Dipartimento di Fisica, Università di Roma "La Sapienza",*

*P.zle A. Moro 2, I-00185 Roma, Italy*

<sup>2</sup> *INFM-CRS SOFT, Università di Roma "La Sapienza",*

*P.zle A. Moro 2, I-00185, Roma, Italy.*

<sup>3</sup> *Dipartimento di Fisica, Università di Perugia,*

*v. A. Pascoli, I-06123 Perugia, Italy*

(Dated: November 20, 2018)

## Abstract

The phase diagram of a charged colloidal system (Laponite) has been investigated by dynamic light scattering in a previously unexplored range of salt and clay concentrations. Specifically the clay weight and salt molar concentrations have been varied in the ranges  $C_w = 0.004 \div 0.025$ ,  $C_s = (1 \times 10^{-3} \div 5 \times 10^{-3})$  M respectively. As in the case of free salt water samples ( $C_s \simeq 1 \times 10^{-4}$  M) an aging dynamics towards two different arrested phases is found in the whole examined  $C_w$  and  $C_s$  range. Moreover a transition between these two different regimes is found for each investigated salt concentration. It is clear from these measurements that a revision of the phase diagram is necessary and a new "transition" line between two different arrested states is drawn.

PACS numbers: 82.70.Dd, 82.70.Gg, 61.20.Lc, 78.35.+c

## I. INTRODUCTION

In spite of intensive research on Laponite clay suspensions in water, motivated by its intriguing properties and important industrial applications, a general agreement about its phase diagram is still lacking. It is however clear that a very rich phenomenology appears varying clay concentration ( $C_w$ ) and/or salt concentration ( $C_s$ ) in the system. Broadly speaking the phase diagram [1] shows that at relatively low salt concentration, increasing clay weight one can obtain a liquid phase, a gel (or glass) phase and a nematic gel, at high salt concentrations one instead observes flocculation. The most studied part of the phase diagram is the one at low salt concentration (usually samples are prepared in pure deionized water,  $C_s \simeq 1 \times 10^{-4}M$ ) and intermediate clay concentration ( $C_w \simeq 3\%$ ). In this region several dynamical light scattering measurements have shown that the samples initially liquids age towards an arrested phase [2, 3, 4, 5, 6] but the mechanism of aggregation is not clear. The gel/glass state has been in fact attributed by different authors to Wigner glass transition [3], frustrated nematic transition [1, 7, 8, 9], micro-segregation [1, 10, 11], gelation [12, 13, 14], etc.. Moreover recent investigations have shown that also the low salt/low clay concentration region of the phase diagram is very interesting and that this is not a region of stable liquid phase as previously supposed. In particular, by dynamic and static light scattering measurements, an arrested phase has been surprisingly found also at low clay concentrations for very long waiting times [12, 13, 14, 15, 16]. Therefore it is clear that the previously proposed phase diagrams [1, 18, 19] need to be revised also in the low clay/low salt concentration region [14]. Moreover the understanding of the physical mechanism that can originate an arrested phase also at clay concentration so low as  $C_w=0.3\%$  and with no added salt is particularly intriguing. In our previous works we have speculated about the origin of the arrested phases in low and intermediate clay concentration in salt free deionized water [15, 16]. In this paper we want to extend our measurements performing the same systematic study as a function of clay concentration but introducing salt in the solutions to change its ionic strength. In particular we want to investigate an unexplored region of the phase diagram focusing our attention at low clay but higher salt concentrations and across the supposed liquid/gel transition of Mourchid et al.[1]. A very recent paper [17] has investigated very dilute Laponite solutions at two different salt concentrations with static light scattering and small-angle x-ray scattering techniques but at the moment there

are not dynamic light scattering data that are spanning in a complete way this region of the phase diagram (there are not available data at  $I \geq 10^{-3}M$  [19]) and these measurements can be very useful to understand the intriguing and controversy Laponite phase diagram.

In this paper we observe that for all the samples studied, for all clay concentrations (up to very low one,  $C_w = 0.3\%$ ) and all salt concentrations ( $C_s = 1 \times 10^{-3}M$ ,  $C_s = 2 \times 10^{-3}M$ ,  $C_s = 5 \times 10^{-3}M$ ), the liquid phase is not the stable one but the samples age toward an arrested phase. These results confirm the previous ones about the arrested phase found at very low clay concentrations in pure water[15, 16]. The time necessary for the sample to evolve in an arrested state depends on clay and salt concentrations, as we will see later. For none of the samples studied we have found flocculation, also at the highest studied salt concentration, in agreement with previous results [1, 14].

## II. EXPERIMENTAL SECTION

### A. Materials

Laponite RD is produced by Laporte Industries with a density of  $2570 \text{ Kg/m}^3$ . It is composed of rigid disc-shaped crystals with a well defined thickness of 1 nm and an average diameter of about 30 nm. Each crystal is composed of roughly  $\sim 1500$  unit cells with an empirical chemical formula  $Na_{0.7}^+[(Si_8Mg_{5.5}Li_{0.3})O_{20}(OH)_4]^{-0.7}$ . The cell structure is a layer of six octahedral magnesium ions sandwiched between two layers of four tetrahedral silicon atoms that are bonded with  $Na$  atoms.

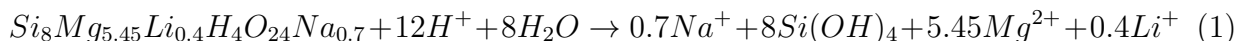
When the powder is dispersed in water, the  $Na^+$  ions on the surface are released and a strongly negative charge (roughly 700 elementary charge) appears on the faces. On the other hand, because of the protonation of the OH groups with the hydrogen atoms of water, a weakly positive charge appears on the rim of the discs.

### B. Samples Preparation

Laponite powder was dried at  $T = 400 \text{ K}$  for 4 hours because up to 20% of its "as prepared" weight is due to adsorbed water. Then the powder is dispersed in a solution of NaCl at the desired salt concentrations  $C_s$ , prepared by adding salt to MilliQ deionized water ( $18 \text{ M}\Omega$ ,  $pH = 7$ ) in different weight proportions to obtain  $C_s = 1 \times 10^{-3}M$ ,  $C_s = 2 \times 10^{-3}M$

and  $C_s = 5 \times 10^{-3}M$ . Laponite dispersion was stirred vigorously until the sample become transparent and finally filtered through a  $0.45 \mu m$  pore size Millipore filters. The starting aging (or waiting) time ( $t_w=0$ ) is defined as the time when the suspension is filtered.

Chemical dissociation of Laponite platelet is an important phenomenon, that -if present- could seriously affect the behavior of the samples. From data available in literature it is in fact known that Laponite dissociation is actually present in acid solutions, that could be the result, for example, of leaving samples in contact with atmospheric  $CO_2$ . The chemical reaction of this dissociation is [21, 22]:



It is evident from this reaction that the eventual platelet dissociation would be signaled by the presence of  $Mg^{++}$  ions in solution. To avoid this phenomenon, our samples were prepared with particular care, preventing any contact with air during and after sample preparation (the samples have been prepared in a glove box under nitrogen atmosphere, and then sealed in quartz cells). Another important chemical modification could be due to the change with aging time of the amount of  $Na^+$  ions in solution. It is in fact well know that at the early stage of the solution,  $Na^+$  ions detaches from the Laponite surfaces and establish the ionic strength of the solution.

We are confident that no chemical modifications of the solutions take place after the first 10-20 minutes because after Laponite is suspended in pure water the pH of the solution, measured by a Crison Glp 22 pHmeter, reached in few minutes a value in the range  $pH=9.8\div 10.0$ . The pH was then monitored in part of the sample left in the glove box under nitrogen atmosphere and we did not observe any deviance from this value also on a time scale of weeks or months. Moreover, a set of measurements aiming to determine the ratio, for both  $Na^+$  and  $Mg^{++}$ , of ions dissolved in the solution (characterized by a narrow NMR absorption line) to those stuck in the solid environment of the platelet (broad NMR absorption band) has been performed on the same samples [23]. These measurements show that the fraction of solvated  $Na^+$  ions does not change with time, and that the solvated  $Mg^{++}$  ions are absent. Therefore, we are confident that Laponite dissolution is not present in our samples.

A large number of Laponite dispersions at several salt concentrations have been prepared: for  $C_s = 1 \times 10^{-3}M$ ,  $C_s = 2 \times 10^{-3}M$ , and  $C_s = 5 \times 10^{-3}M$ . The samples investigated

are indicated by dots in the  $C_s - C_w$  phase diagram reported in Figure 1, also indicated are the samples previously studied [15, 16] in pure deionized water ( $C_s \simeq 1 \times 10^{-4}M$ ). In the following we will name the samples reported in the figure as open circles as "low" concentration samples while samples reported as full circles as "high" concentration samples for the reasons discussed below.

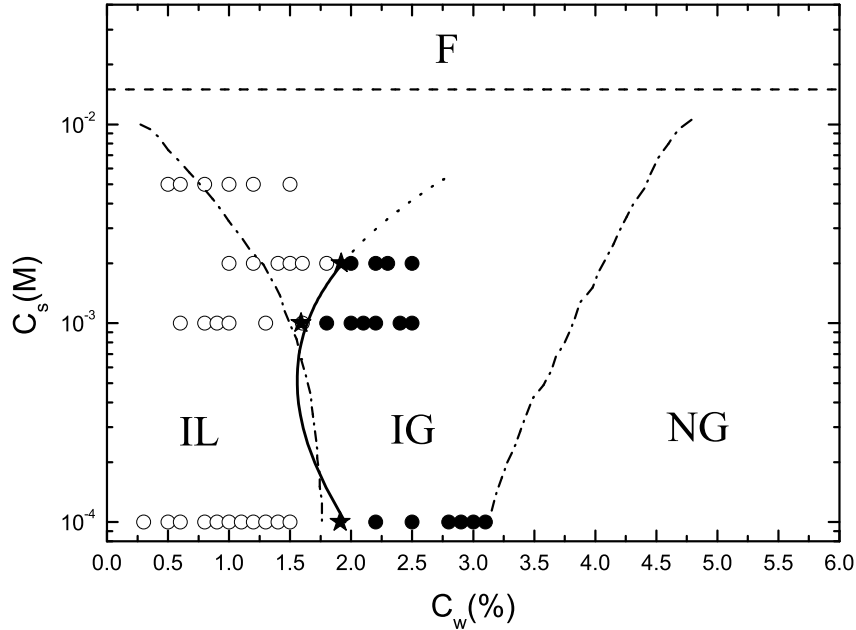


FIG. 1:  $C_s - C_w$  phase diagram proposed in Ref.[1]. The isotropic liquid (IL)-isotropic gel (IG) and isotropic gel (IG)-nematic gel (NG) transition lines from [1] are reported as dashed-dotted lines. The dashed line in the upper part of the diagram separates the flocculation region (F). Open and full circles indicate respectively "low" and "high" concentration samples measured in the present work. The stars indicate the concentration values obtained from the fit analysis of Fig. 4 while the thick full-dotted curve drawn from these points represents the new line proposed that marks the transition between the two different aging behaviors. Both at the left and right of this line the system is arrested and form an isotropic gel. The last part of the line is dashed because at the highest studied salt concentration ( $C_s = 5 \times 10^{-3}M$ ) the aging dynamics at clay concentration larger than  $C_w = 1.5 \%$  is too fast to be followed with photoncorrelation measurements. Data at  $C_s = 1 \times 10^{-4}M$  are from our previous works[15, 16].

### C. Equipment and Measurements

Dynamic light scattering measurements were performed using an ALV-5000 logarithmic correlator in combination with a standard optical setup based on an He-Ne ( $\lambda = 632,8 \text{ nm}$ ) 10 mW laser and a photomultiplier detector. The intensity correlation function was directly obtained as:

$$g_2(q, t) = \frac{\langle I(q, t)I(q, 0) \rangle}{\langle I(q, 0) \rangle^2}, \quad (2)$$

where  $q$  is the modulus of the scattering wave vector defined as  $q = (4\pi n/\lambda) \sin(\theta/2)$  with  $\theta = 90^\circ$  in this experiment. The dynamic structure factor  $f(q, t)$  can be directly obtained inverting the Siegert relation :

$$f(q, t) = \sqrt{\frac{g_2(q, t) - 1}{b}}. \quad (3)$$

where  $b$  represents the coherence factor.

## III. RESULTS AND DISCUSSION

### A. The aging phenomenon in Laponite suspensions

According to the phase diagram obtained from Mourchid *et al.*[1] up and below a certain concentration  $C_w^*$ , that depends on salt concentration  $C_s$ , Laponite suspensions can be in two different physical states. Low concentration suspensions ( $C_w < C_w^*(C_s)$ ) should form stable, equilibrium liquid phase (**IL** phase of Fig. 1). Higher concentration suspensions ( $C_w > C_w^*(C_s)$ ) are initially fluids but experience aging and pass into an arrested phase after a time that depends on the clay amount and salt concentration (**IG** phase of Fig. 1). However, as already discussed, recent investigations have shown that the phase diagram needs to be revised. In particular, a surprising arrested phase has been found also at low clay concentrations (well within the supposed stable **IL** phase of Fig. 1) for very long waiting times [12, 13, 14, 15, 16].

Correlation functions at increasing waiting times  $t_w$  for four samples at two different salt concentrations  $C_s$  are reported in Figure 2 as an example. In particular low ( $C_w = 0.6\%$  - panel (A)) and high ( $C_w = 2.0\%$  - panel (B)) clay concentration samples for  $C_s = 1 \times 10^{-3} M$  and low ( $C_w = 1.0\%$  - panel (C)) and high ( $C_w = 2.5\%$  - panel (D)) clay concentration

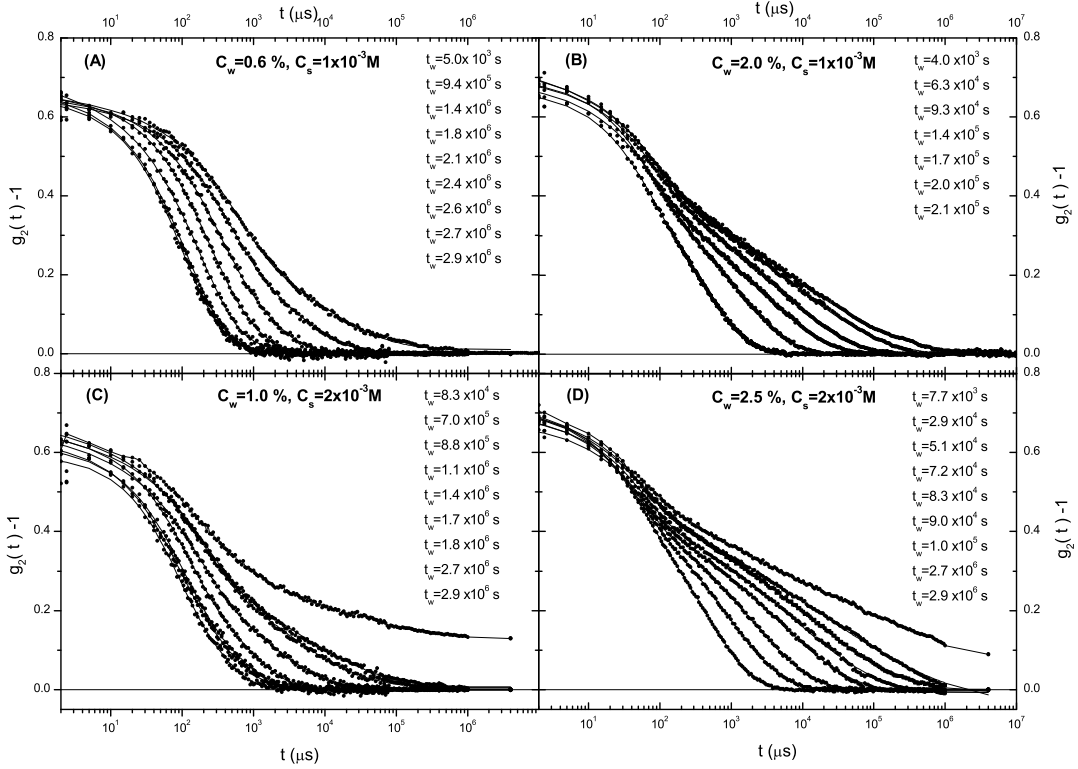


FIG. 2: Evolution of the measured intensity correlation functions (symbols) and corresponding fits with Eq. (4) (continuous lines) for four different Laponite suspensions  $C_w$  at two salt concentrations  $C_s$ . For  $C_s = 1 \times 10^{-3} M$ :  $C_w=0.6\%$  (A) and  $C_w=2.0\%$  (B). For  $C_s = 2 \times 10^{-3} M$ :  $C_w=1.0\%$  (C) and  $C_w=2.5\%$  (D). The curves are measured at increasing waiting times (indicated in the figure) from left to right. In panels (C) and (D) also the transition in the non ergodic phase are reported.

samples for  $C_s = 2 \times 10^{-3} M$  are shown. It is evident from the figure that all the samples are actually performing aging and that the liquid phase is not the stable one. The evolution of the spectra with the waiting time (aging) is in fact evident. The crossover from a complete to incomplete decay of the correlation function (indication of a transition towards a non ergodic, arrested, state) is also reported as an example in the lower panel of Fig. 2. Only the ergodic spectra of each sample have been studied in the paper. As for the samples prepared in pure water, the correlation functions (Figure 2) decay following a two steps behavior (more evident from panels B and D of the figure) and for this reason we apply

to these measurements the same data analysis used previously [15, 16]. The two different decaying, the fast and the slow ones, can be described quantitatively assuming for  $f(q, t)$  a time dependence given by the weighted sum of two contributions, a simple exponential to represent the fast decay (weight  $a$ ) and a stretched one [ $e^{-(t/\tau_2)^\beta}$ ] for the slow decay (weight  $(1 - a)$ ). The measured quantity,  $g_2(q, t) - 1$ , is thus the squared sum of the two terms:

$$g_2(q, t) - 1 = b \left( a e^{-t/\tau_1} + (1 - a) e^{-(t/\tau_2)^\beta} \right)^2. \quad (4)$$

The fits with Eq. 4 well describe the data as can be seen from the full lines superimposed to the experimental points reported as an example in Figure 2.

Directly from the raw spectra reported in Fig 2 it is already possible to observe as the evolution with waiting time is qualitatively different for low and high concentration samples, as also observed in free salt samples [15, 16]. While in fact for low concentration samples (open circles of Fig 1) (Fig 2A for  $C_s = 1 \times 10^{-3} M$  and Fig 2C for  $C_s = 2 \times 10^{-3} M$ ) one observes the evolution with  $t_w$  of the whole  $g_2 - 1$ , i.e. both the fast ( $\tau_1$ ) and the slow ( $\tau_2$ ) decays evolve with  $t_w$ , for the higher concentration samples (full circles of Fig. 1) (Fig 2B for  $C_s = 1 \times 10^{-3} M$  and Fig 2D for  $C_s = 2 \times 10^{-3} M$ ) the fast decay remains essentially constant while the slow one becomes larger and larger when the waiting time increases. This qualitative observation is fully confirmed by the data analysis (see below).

## B. The slow dynamics: the B parameter and the aggregation rate

We will focus now our attention on the slow dynamics and its characteristic parameters.

One can think to the stretched exponential as the results of the superposition of single exponentials:

$$e^{-(t/\tau_2)^\beta} = \int_0^\tau \phi_{\tau_2, \beta}(\tau') e^{-t/\tau'} d\tau' \quad (5)$$

where  $\phi_{\tau_2, \beta}(\tau)$  is the appropriate distribution of relaxation times  $\tau$  (this distribution function has not an expression in terms of elementary functions).

From the correlation time  $\tau_2$  and the stretching exponent  $\beta$  it is then possible to define the mean relaxation time  $\tau_m$  of the distribution  $\phi$  that gives rise to the stretched exponential form:

$$\tau_m = \int_0^\tau \tau' \phi_{\tau_2, \beta}(\tau') d\tau' = \tau_2 \frac{1}{\beta} \Gamma\left(\frac{1}{\beta}\right). \quad (6)$$

where  $\Gamma$  is the Euler gamma function.



The value of the mean relaxation time  $\tau_m$  is larger than  $\tau_2$  and it spans more decades, because of the  $t_w$  dependence of  $\beta$ , but the qualitative behavior of the two relaxation times is the same. Indeed both  $\tau_2$  and  $\tau_m$  seem to diverge at a given waiting time  $t_w^\infty$  i.e. when the system is arrested. This behavior is evident from Fig. 3 of Ref.[16] where the comparison between  $\tau_2$  and  $\tau_m$  for several samples is reported.

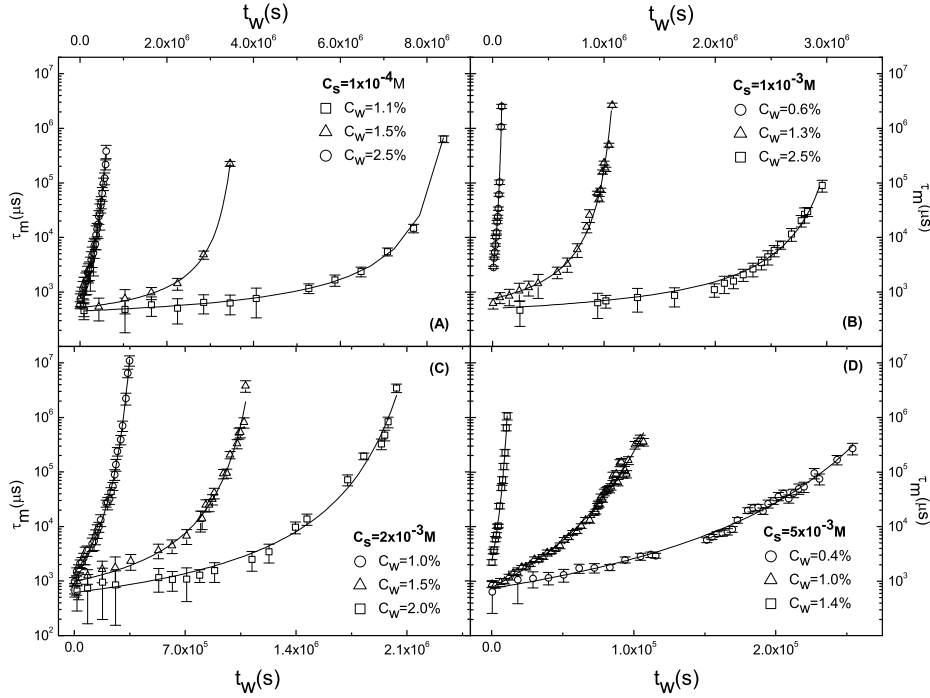


FIG. 3: Waiting time dependence of  $\tau_m$  and relative fits according to Eq. 7 for several sample concentrations  $C_w$  at different salt concentrations  $C_s$ . (A):  $C_w=1.1$ ; 1.5 and 2.5 % for  $C_s \simeq 1 \times 10^{-4}$  M from Ref.[15]. (B):  $C_w=0.6$ ; 1.3 and 2.5 % for  $C_s = 1 \times 10^{-3}$  M. (C):  $C_w=1.0$ ; 1.5 and 2.0 % for  $C_s = 2 \times 10^{-3}$  M. (D):  $C_w= 0.4$ ; 1.0 and 1.4 % for  $C_s = 5 \times 10^{-3}$  M.

In Fig. 3 the values of  $\tau_m$ , calculated according to Eq. 6, for several clay concentrations at the four studied salt concentrations are reported as examples.

We observe that in the region of times studied in this paper  $\tau_2$  (or equivalently  $\tau_m$ ) is always much smaller than  $t_w$ , this indicating that the measured  $g_2$  are well defined quantities. We clearly observe that the dependence of  $\tau_m$  on the waiting time  $t_w$  is faster than exponential. This is not in contradiction with previous results because the deviation from

the exponential growth is clearly noticeable only at low clay concentrations, where there are not data available in literature. At high clay concentration the simple exponential shape can be confused with our faster than exponential behavior.

For a quantitative analysis, we represent the aging time dependence of relaxation times as [15, 16]:

$$\tau_m = \tau_m^0 \exp\left(B \frac{t_w}{t_w^\infty - t_w}\right) \quad (7)$$

This equation is not derived from any first principle argument, rather it embodies the exponential growth of the  $\tau_m$  for short  $t_w$  (as previously observed [6, 19, 24]) and the existence of a divergence of  $\tau_m$  at a finite value of  $t_w$ , i.e.  $t_w^\infty$ .

Equation 7 well describes the measurements as can be seen from the fit curves reported as continuous lines in Fig 3.

The parameters of the fits,  $B$  and  $t_w^\infty$ , in function of Laponite concentration  $C_w$  at the different salt concentrations studied are reported in Fig. 4 and 5. Salt concentration is decreasing from the top (A) to the bottom (D) of the figures where panel D reports our data in pure deionized water [15, 16].

It is evident from figure 4 that the results found previously for the free salt suspensions are confirmed: the  $B$  parameter, that measures how fast  $\tau_m$  approaches the divergence, is almost constant for all the samples at low concentration and drifts towards a higher, again constant, value for high concentration samples. This happens for all the series of studied samples, from the lowest to the highest values of salt concentrations. In the discussion of Fig. 2 we already observed that the aging process is qualitatively different for the low and high concentration samples. Figure 4 quantify this difference in the physical properties characterizing the aging phenomenon in the two different concentration regions. From the behavior of the  $B$  parameter reported in this figure it is evident that the existence of two different routes toward an arrested phase found for the samples at  $C_s \simeq 1 \times 10^{-4} M$  [15, 16] is also present for this new series of samples with higher ionic strength. The transition between the low and the high  $B$  values should indicate a transition line between the two different routes to gelation. The position of this line depends on salt concentration. In Fig. 4 a fit of the  $B$  parameter for each salt concentration with a sigmoid curve is also reported. From this fit analysis is possible to extract the mean concentration value of the transition, and this gives an indication of the transition line. These values are reported as stars in Fig. 1

In Fig. 5 the behavior of the  $t_w^\infty$  parameter in function of the clay concentration  $C_w$

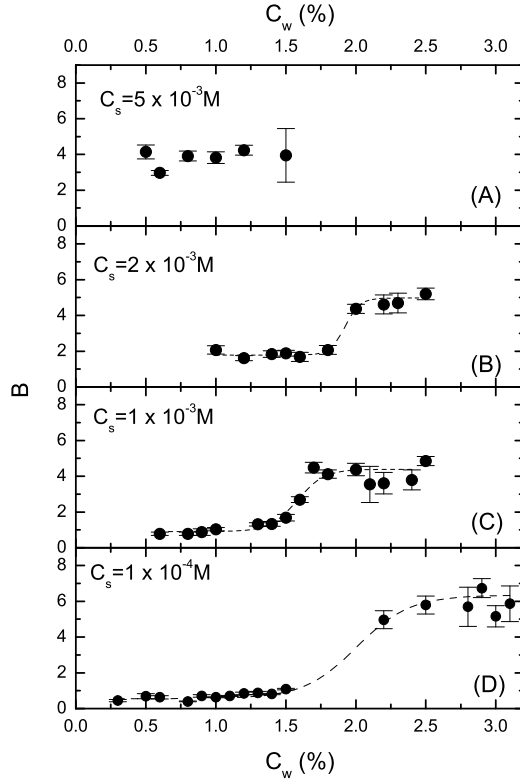


FIG. 4: Concentration dependence of the  $B$  parameter for all the samples at the indicated salt concentrations decreasing from top (panel A) to bottom (panel D). Data reported in panel D are from our previous measurements [15, 16]. The transition from a constant value for the low concentration samples towards another constant value for the high concentration samples (reported respectively as open and full circles in Fig 1) is an indication of a transition between two different arrested states. The line reported in the figure is a sigmoidal fit of the  $B$  parameter.

for different salt values is reported. We can observe that for each sample at each salt concentration the  $t_w^\infty$  parameter actually exists and is finite; this is the indication that all the studied samples are not in a stable phase but evolve with waiting time toward an arrested state. The value of  $t_w^\infty$  changes with clay and salt concentration. At fixed salt concentration  $C_s$  it decreases at increasing Laponite concentration  $C_w$ , in agreement with the fact that more the sample is concentrated faster is the aggregation process.  $t_w^\infty$  generally decreases also with increasing salt concentration  $C_s$  (passing from panel D to panel A), in particular it is strongly decreased going from  $C_s \simeq 1 \times 10^{-4} M$  to  $C_s = 1 \times 10^{-3} M$ , it is essentially

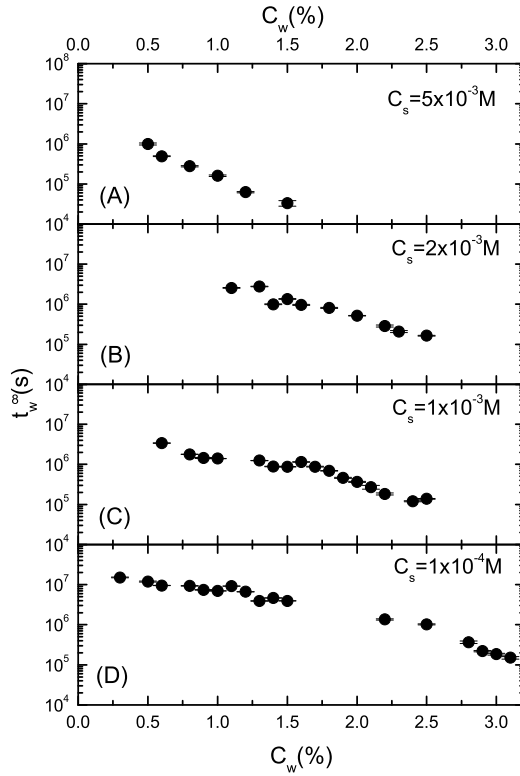


FIG. 5: Concentration dependence of the divergence time  $t_w^\infty$  for all the samples at the indicated salt concentrations decreasing from top (panel A) to bottom (panel D). Data reported in panel D are from our previous measurements [15, 16].

constant going to  $C_s = 2 \times 10^{-3} M$ , and it is again strongly reduced for  $C_s = 5 \times 10^{-3} M$ . Also this behavior is in agreement with the fact that the aggregation is faster for the samples with higher salt concentration. It must be emphasized that  $t_w^\infty$  is smooth and continuous with  $C_w$ , and it does not show any signature of the transition concentration, where  $B$  is discontinuous.

### C. The hypothesized phase diagram for low concentrations sample

From the measurements reported in this paper and from that reported in free salt water [15, 16] we can now draw an alternative phase diagram for Laponite solutions. At variance with the results of [1, 18] it is definitely clear that the low clay concentration region of the phase diagram is neither a liquid neither a sol stable phase, both at low salt concentration

( $C_s \simeq 10^{-4}M$ ) and at higher salt concentration. The state of the system depends on time and the very long waiting time necessary to obtain the arrested phase (especially at low salt low clay concentrations) can be the reason because previous studies have believed the initial liquid phase to be the stable one. In regard of this point we can observe from Fig. 5 that for all the different salt concentrations the parameter  $t_w^\infty$  increases in a continuous way as clay concentration is decreased (as already discussed). Therefore we believe that also the samples found in a liquid phase from Ref. [14], will transit in an arrested phase for a long enough waiting time. This time can be obtained by an extrapolation at the interested clay concentration of the  $t_w^\infty$  reported in Fig. 5 and, for example, for  $C_s = 1 \times 10^{-3}M$  it results to be around 3 months or more for a clay concentration of  $C_w = 0.3 \%$ . However, due to the lack of information on this low  $C_w$  region, we cannot exclude the possibility that at low enough concentration a really stable liquid phase actually exists.

From the behavior of the B parameter reported in Fig. 4 we can also state that in the high clay concentration region no discontinuity is found increasing salt concentration from  $C_s = 1 \times 10^{-4}M$  up to  $C_s = 5 \times 10^{-3}M$  while a general slow decrease of the "high" value of the B parameter is found. This is an important issue that enters in the discussion about the origin of the arrested phase at  $C_s = 1 \times 10^{-4}M$  as glass or gel phase [14, 18]. Our measurements are of dynamic type so we cannot access the structure factor of the samples and we cannot distinguish in this sense between the gel and the glass phase but we can say that there is not any discontinuity between  $C_s = 1 \times 10^{-4}M$  and higher salt concentrations. For this reason the arrested phase existing in free salt water should persist also adding salt to the solutions. Relying on the fact that for  $C_s > 1 \times 10^{-3}M$  the origin of the arrested phase is universally assigned to gelation [14, 18], we conclude that the same gel phase should be present at  $C_s = 1 \times 10^{-4}M$ .

Also the low clay concentration phase (low values of the B parameters) has no signs of discontinuity, nevertheless the "low" value of the B parameter increases at increasing salt concentration.

For these reasons moving vertically in the phase diagram, i.e. fixing a clay concentration value and increasing salt concentration, one finds a continuous evolution of the B parameter both at low and at high clay concentrations.

The behavior is completely different if we span horizontally the phase diagram, i.e. if we fix salt concentration and increase clay concentration. For all the different salt concentration

values we find a discontinuity in the B value and a drift from a "low" to a "high" value of this parameter. Therefore we have found again, as already seen in free salt water, the existence of two different routes to reach the arrested phase, for low and high clay concentration. The fit analysis of Fig 4 permits also to obtain an estimation of the concentration value that represents the transition point between the two different arrested states. In this way we can draw a new transition line in the phase diagram between two different arrested phases. This is reported as full-dotted line in Fig. 1.

As already said before we cannot have a direct evidence of the gel/glass origin of the non ergodic phases but we can speculate that the arrested phase at low clay concentration is originated from clusters of Laponite while single Laponite disks directly participate to the formation of the arrested phase at higher clay concentration.

#### IV. CONCLUSIONS

From our previous work about Laponite dispersions in salt free deionized water we have shown the presence of an arrested phase at very low clay concentration and the existence of two different routes to reach the aggregated phase for "low" and "high" clay concentration [15, 16]. In this paper we have investigated the effect of increasing the ionic strength of a water dispersion of Laponite. Systematic measurements at three different values of salt concentrations have been in fact performed and these data give now information on a wide part of Laponite solutions phase diagram. The results obtained have undoubtedly confirmed the existence of an arrested phase at low clay concentration for each salt concentration. Moreover the measurements have also validated the goodness of the proposed analysis for samples in pure deionized water and the existence of two different aggregation mechanisms. In particular at the fixed clay concentration  $C_w = 3 \%$  no discontinuity is found increasing salt concentration, thus confirming the hypothesis of a gel phase in the whole ionic strength range proposed in Ref.[14]. On the contrary at each salt concentration investigated here, increasing clay concentration a transition line between two different aggregated phases is

found.

- 
- [1] Mourchid, A.; Delville, A.; Lambard, J.; Lècolier, E.; Levitz, P. *Langmuir* **1995**, *11*, 1942-1950.
  - [2] Kroon, K.; Wegdam, G.H.; Sprik, S. *Phys. Rev. E* **1996**, *54*, 6541-6550.
  - [3] Bonn, D.; Tanaka, H.; Wegdam, G.; Kellay, H.; Meunier, J. *Europhys. Lett.* **1998**, *45*, 52-57.
  - [4] Knaebel, A.; Bellour, M.; Munch, J-P.; Viasnoff, V.; Lequeux, F. ; Harden, J.L.; *Europhys. Lett.* **2000**, *52*, 73-79.
  - [5] Abou, B.; Bonn, D.; Meunier, J. *Phys. Rev. E* **2001**, *64*, 21510-21516.
  - [6] Bellour, M.; Knaebel, A.; Harden, J.L.; Lequeux, F.; Munch, J-P.; *Phys. Rev. E* **2003**, *67*, 31405-31408.
  - [7] Kroon, M.; Vos, W.L.; Wegdam, G.H. *Phys. Rev. E* **1998**, *57*, 1962-1970.
  - [8] Gabriel, J.C.P.; Sanchez, C.; Davidson, P. *J. Phys. Chem.* **1996**, *100*, 11139-11143.
  - [9] Mourchid, A.; Lècolier, E.; Van Damme, H.; Levitz, P. *Langmuir* **1998**, *14*, 4718-4723.
  - [10] Pignon, F.; Magnin, A.; Piau, J.M.; Cabane, B.; Lindner, P.; Diat, O. *Phys. Rev. E* **1997**, *56*, 3281-3289.
  - [11] Martin, C.; Pignon, F.; Piau, J.M.; Magnin, A.; Lindner, P.; Cabane, B. *Phys. Rev. E* **2002**, *66*, 21401-21411.
  - [12] Nicolai, T.; Cocard, S. *J. Colloid Interface Sci.* **2001**, *244*, 51-57.
  - [13] Nicolai, T.; Cocard, S. *Eur. Phys. J. E* **2001**, *5*, 221-227.
  - [14] Mongondry, P.; Tassin, J.F.; Nicolai, T. *J. Colloid Interface Sci.* **2005**, *283*, 397-405.
  - [15] Ruzicka, B.; Zulian, L.; Ruocco, G. *Phys. Rev. Lett.* **2004**, *93*, 258301-258305.
  - [16] Ruzicka, B.; Zulian, L.; Ruocco, G. *J. of Phys. Cond. Matt.* **2004**, *16*, S4993.
  - [17] Li, L.; Harnau, L.; Rosenfeldt, S.; Ballauff, M. *cond-mat/0508034*.
  - [18] Tanaka, H.; Meunier, J.; Bonn, D. *Phys. Rev. E* **2004**, *69*, 31404-31410.
  - [19] Tanaka, H.; Meunier, J.; Bonn, D. *Phys. Rev. E* **2005**, *71*, 21402-21412.
  - [20] Tawari, S. L.; Koch, D. L.; Cohen, C. *J. Colloid Interface Sci.* **2001**, *240*, 5466.
  - [21] Thompson, D.W.; Butterworth, J.T. *J. Colloid Interface Sci.* **1991**, *151*, 236-243.
  - [22] Mourchid, A.; Levitz, P. *Phys. Rev. E* **1998**, *57*, R4887.
  - [23] Capuani, S.; Gili, T.; Maraviglia, B. *preprint*.

- [24] Kaloun, S.; Skouri, R.; Skouri, M.; Munch, J. P.; Schosseler, F. *Phys. Rev. E* **2005**, *72*, 11403-11408.